ELSEVIER

Materials Science and Engineering C 11 (2000) 41–46

MATERIALS SCIENCE & ENGINEERING C

www.elsevier.com/locate/msec

Orientation and loading condition dependence of fracture toughness in cortical bone

Zude Feng [a,*], Jae Rho [b], Seung Han [c], Israel Ziv [c]

[a] *Department of Materials Science, Xiamen University, Xiamen 361005, People's Republic of China*
[b] *Department of Biomedical Engineering, University of Memphis, Memphis, TN 38152, USA*
[c] *Department of Orthopaedic Surgery, State University of New York at Buffalo, Buffalo, NY 14214, USA*

Received 1 July 1999

Abstract

The fracture toughness at crack initiation were determined for bovine cortical bone under tension (mode I), shear (mode II), and tear (mode III). A total of 140 compact tension specimens, compact shear specimens and triple pantleg (TP) specimens were used to measure fracture toughness under tension, shear, and tear, respectively. Multiple-sample compliance method was utilized to measure the critical strain energy release rate (G_c) at the $a/W = 0.55$ (crack length, a, to specimen width, W, ratio). The critical stress intensity factor (K_c) was also calculates from the critical loading (P_c) of the specimens at the $a/W = 0.55$. The effect of the anisotropy of bone on its resistance to crack initiation under shear and tear loading was investigated as well. Fracture toughness of bone with precrack orientations parallel (designed as longitudinal fracture) and vertical (designed as transverse fracture) to the longitudinal axis of bone were compared. In longitudinal fracture, the critical strain energy release rate (G_c) of cortical bone under tension, shear, and tear was 644 ± 102, 2430 ± 836, and 1723 ± 486 N/m, respectively. In transverse fracture, the critical strain energy release rate (G_c) of cortical bone under tension, shear, and tear was 1374 ± 183, 4710 ± 1284, and 4016 ± 948 N/m, respectively. An unpaired t-test analysis demonstrated that the crack initiation fracture toughness of bone under shear and tear loading were significantly greater than that under tensile loading in both longitudinal and transverse fracture ($P < 0.0001$ for all). Our results also suggest that cortical bone has been ''designed'' to prevent crack initiation in transverse fracture under tension, shear, and tear. © 2000 Elsevier Science S.A. All rights reserved.

Keywords: Fracture toughness; Cortical bone; Tension; Shear; Tear

1. Introduction

An overall understanding of initiation and propagation of cracks in cortical bone may contribute to our capability of prediction and reduction of the fracture risk of bone resulted from aging, incident, or repeated loading. However, the majority of our understanding about the phenomena has focused on its resistance to initiation and propagation of cracks under tension [1–3]. Actually, long bone, which has irregular shape and anisotropic mechanical properties, is usually subjected to a combined load in daily physiological activities. Accordingly, cracks in bone, which are randomly oriented with respect to the loading axis of bone, seldom experience pure tensile loading. The conditions for criticality to failure may vary considerably from those predicted by tensile loading parameters in most cases. In general, initiation and propagation of fracture cracks in bone can occur under three basic loading modes and their combinations at the tip of the cracks, namely, tensile (mode I), shear (mode II), and tear (mode III), tensile + shear, tensile + tear, and shear + tear, respectively. Thus, the characterization of crack growth fracture toughness under shear and tear is required (Fig 1).

Recently, Norman et al. [4] reported their investigation of the resistance of human bone to longitudinal fracture (defined as crack propagation parallel to the longitudinal axis of the bone) under shear. However, transverse fracture, defined as crack propagation normal to the longitudinal axis of the bone, is one of the common fracture modes

* Corresponding author. Tel.: +86-592-2183904; fax: +86-592-2189354.
E-mail address: zdfeng@jingxian.xmu.edu.cn (Z. Feng).

0928-4931/00/$ - see front matter © 2000 Elsevier Science S.A. All rights reserved.
PII: S0928-4931(00)00142-9

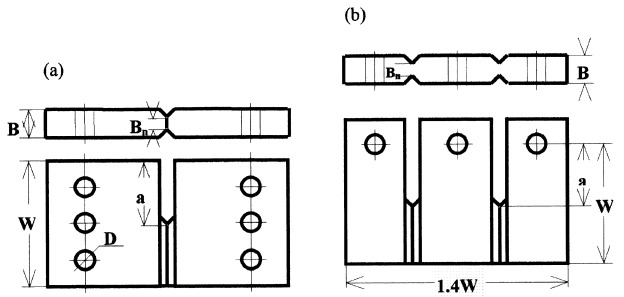

Fig. 1. Specimen design for (a) mode II fracture toughness testing and (b) mode III fracture toughness testing.

of cortical bone [5,6]. In micro level, bone can be simulated as a composite with oriented arranged osteons as fiber reinforced phase. Bone exhibits obvious anisotropic properties in tensile, compressive strength, and elastic modulus due to its specific microstructure [7]. The anisotropic fracture properties of bone under tensile loading have been well-documented [6]. The resistance of bone to transverse fracture under shear and tear loading has not been measured.

The purpose of the present study was to investigate: (1) the resistance of cortical bone to crack initiation under tensile, shear, and tear loading; (2) the orientation dependence of the resistance of bone to fracture under shear and tear loading.

2. Experimental

A total of 140 compact tension, compact shear, and TP specimens were used to measure fracture toughness of cortical bone under tension, shear, and tear. Specimens were machined under water irrigation from the lateral and medial cortices of fresh adult bovine femora exhibiting predominantly secondary osteons. Among the 140 specimens, 40 compact tension specimens [6], 50 compact shear specimens [8,9], and 50 TP specimens [10,11] were used to measure critical stress intensity factor (K_c), critical strain energy release rate (G_c) under tension, shear, and tear loading, respectively. Mode I, mode II, and mode III fracture toughness tests were conducted in both longitudinal and transverse fracture. All the specimens used in this investigation had the same width ($W = 14$ mm) and thickness ($B = 5$ mm) for comparison. A chevron notch was machined on the specimens according to ASTM E399-83 (1985). The length of the notch was slightly shorter than the designed length of pre-crack. Afterwards, a 1.25 mm deep V-notched groove was machined on both sides of the specimens along the direction of the chevron notch, leaving 2.5 mm thickness between the grooves ($B_n = 2.5$ mm). The specimens were spayed with physiological saline during machining. After machining, the specimens were wrapped in gauze saturated with physiological saline and frozen at -20°C prior to testing.

Prior to mechanical testing, specimens were defrosted in physiological saline. After the temperature of the specimens reached room temperature (25°C) and the specimens were kept under the temperature for 1 h, a precrack was initiated in the chevron notch using a razor blade. The chevron notch and precrack combined were located at a/W (crack length, a, to specimen width, W, ratio) equal to 0.45, 0.55, or 0.65 for mode I compliance specimens and at 0.30, 0.40, 0.55, or 0.70 for mode II and mode III compliance specimens. The test specimens, saturated in physiological saline, were placed in custom-designed fixtures mounted on a mechanical testing machine. Specimens were loaded to broken at a crosshead displacement rate of 0.2 mm min^{-1}. Applied load and crosshead displacement were recorded using a PC based data acquisition system. Compliance (C) calibration curves were calculated for mode I, mode II, and mode III from the inverse slope of the linear portion of the load-displacement curves in the method suggested by Norman et al. [4]. Critical load (P_Q) was determined at the onset of crack growth according to ASTM E399 (1985).

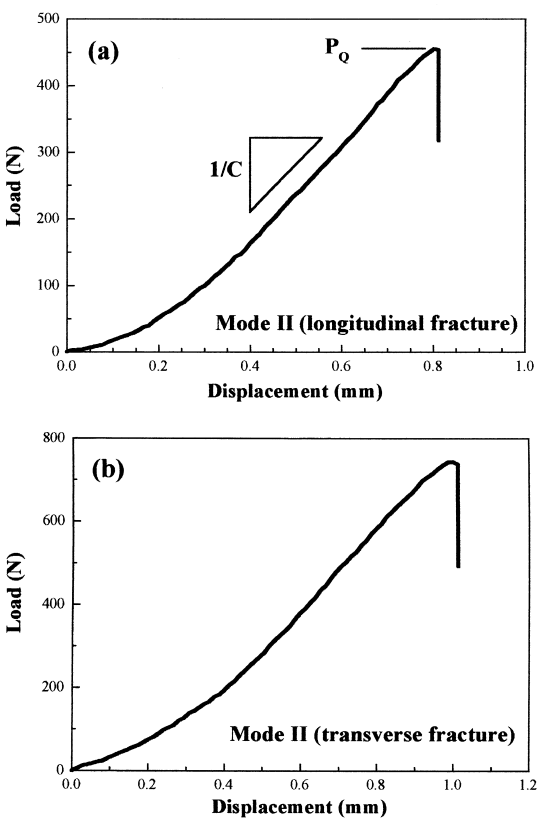

Fig. 2. Representative load vs. load-line displacement plot from mode II tests in (a) longitudinal and (b) transverse fracture.

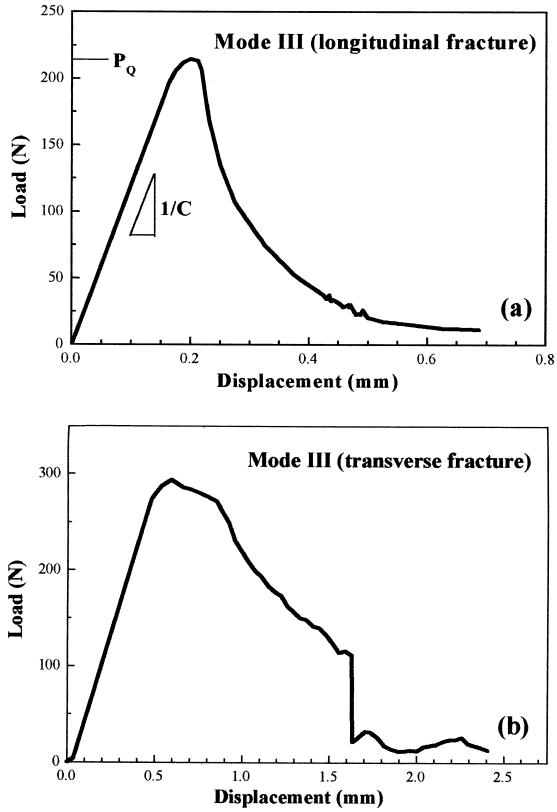

Fig. 3. Representative load vs. load-line displacemnet plot from mode III tests in (a) longitudinal and (b) transverse fracture.

The critical strain energy release rate for mode I (G_{IC}), mode II (G_{IIC}), and mode III (G_{IIIC}) was calculated using the compliance method

$$G_{iC} = \frac{P_Q^2}{2(BB_n)^{1/2}} \frac{\partial C}{\partial a}, (i = \mathrm{I}, \mathrm{II}, \mathrm{III}), \quad (1)$$

where P_Q, B, B_n, and C were defined previously. Effective thickness $(BB_n)^{1/2}$ was used to replace B in the original formula to account for the effect of side grooves [12]. $\partial C/\partial a$ was determined from a fit of experimental compliance. The slopes of the curves $\partial C/\partial a$ and critical load P_Q at $a/W = 0.55$ ($a = 7.7$ mm) were used to calculate G_{IC}, G_{IIC}, and G_{IIIC} from Eq. (1).

The critical stress intensity of mode I (K_{IC}), mode II (K_{IIC}), and mode III (K_{IIIC}) was calculated according to the formula used by Behiri and Bonfield [6], Richard [8], and Kumar et al. [10], respectively.

$$K_{IC} = \frac{P_Q Y}{(BB_n)^{1/2} W^{1/2}}, \quad (2)$$

where

$$Y = 29.6\left(\frac{a}{W}\right)^{1/2} - 185.5\left(\frac{a}{W}\right)^{3/2} + 655.7\left(\frac{a}{W}\right)^{5/2} - 1017\left(\frac{a}{W}\right)^{7/2} + 638.9\left(\frac{a}{W}\right)^{9/2}.$$

$$K_{IIC} = \frac{P_Q}{(BB_n)^{1/2} W} (\pi a)^{1/2} f(a/W), \quad (3)$$

where

$$f(a/W) = \left[\frac{0.16 + 0.68a/(W-a)}{1 - 0.4a/(W-a) + 1.12[a/(W-a)]^2}\right] \Big/ \left(1 - \frac{a}{W}\right).$$

$$K_{IIIQ} = \{P_Q/B_n W^{1/2}\} f(a/W)\, h_{iii}(\phi), \quad (4)$$

where

$h_{iii}(\phi) = 1.2$ in mode III loading.

Each datum was the average of testing results of 5–10 parallel specimens. The data were then subjected to an unpaired *t*-test to investigate the difference of fracture toughness between longitudinal and transverse fracture, and between mode I, mode II, and mode III. Microstructure characterization of fracture surfaces of bone specimens was performed by a Hitachi S-520 scanning electron microscope.

3. Results

Representative load vs. load-line displacement plot obtained from mode II and mode III tests in longitudinal and transverse fracture is illustrated in Figs. 2 and 3, respectively. Linear relationships between compliance (C) and

Table 1
The linear relationships between compliance (C) and crack length (a) for mode I, mode II, and mode III tests

	Mode I			Mode II			Mode III		
	$\partial C/\partial a$	r^2	P	$\partial C/\partial a$	r^2	P	$\partial C/\partial a$	r^2	P
Longitudinal fracture	0.0003628	0.817	< 0.0001	0.000127	0.616	< 0.0001	0.000295	0.717	< 0.0001
Transverse fracture	0.0001943	0.841	< 0.0001	0.000064	0.498	< 0.0001	0.000267	0.446	0.0003

Table 2
Mode I, II, and III fracture toughness of cortical bone in longitudinal and transverse fracture (Average ± S.D.)

	Mode I		Mode II		Mode III	
	G_C (N/m)	K_C (MN m$^{-3/2}$)	G_C (N/m)	K_C (MN m$^{-3/2}$)	G_C (N/m)	K_C (MN m$^{-3/2}$)
Longitudinal fracture	644 ± 102	3.0 ± 0.24	2430 ± 836	6.3 ± 1.2	1723 ± 486	6.5 ± 0.9
Transverse fracture	1374 ± 183	6.0 ± 0.41	4710 ± 1284	12.5 ± 1.7	4016 ± 948	10.5 ± 1.3

crack length (a) for mode I, mode II, and mode III tests in longitudinal and transverse fracture were found to be statistically significant ($P < 0.001$ for all). These were used to determine the slope of the crack growth curves (Table 1). Crack initiation fracture toughness of the bone under tension, shear, and tear loading (G_C and K_C) are shown in Table 2. In longitudinal fracture, both mode II fracture toughness (G_{IIC} and K_{IIC}) and mode III fracture toughness (G_{IIIC} and K_{IIIC}) were statistically significantly greater than mode I fracture toughness (G_{IC} and K_{IC}) ($P < 0.0001$). The average ratios G_{IIC}/G_{IC} and G_{IIIC}/G_{IC} equaled 3.8 and 2.7, respectively. In transverse fracture, both mode II fracture toughness (G_{IIC} and K_{IIC}) and mode III fracture toughness (G_{IIIC} and K_{IIIC}) were statistically significantly greater than mode I fracture toughness (G_{IIIC} and K_{IIIC}) ($P < 0.0001$). The bone revealed anisotropic properties in mode I, mode II and mode III fracture toughness (G_c and K_c) in this study. Fracture toughness for transverse fracture was significantly greater than that in longitudinal fracture under all modes of loading (tensile, shear and tear) ($P < 0.0001$).

The microstructual morphology of the fracture surfaces of the bone specimens are shown in Fig. 4. The fracture surfaces of bone specimens under tear in transverse fracture were rough and uneven in general, revealing the characteristics of partial ''pull-out'' or severe deformation of osteon and lamellae, whereas fracture surfaces of bone specimens under shear in transverse fracture were flat.

4. Discussion

Several methods have been proposed for pure mode II and mode III fracture toughness testing of composite materials [8,10,13–16]. Because of the long bone's curved shape and limited thickness of cortex, compact specimen is more favorable [17] and has been utilized in this study. A 1.25-mm deep V-notched groove was machined on both sides of all specimens in this investigation. It acted as a guide for crack propagation in the transverse fracture [6]. In addition, grooves may increase the stress triaxiality at the edges of the advancing crack as indicated by 3D finite element analysis (FEA) and promote planar crack extension without/with less shear lip formation at the sides of the specimens. This study also suggests that the measure of bone fracture toughness under tear loading using the TP model specimens is adequate for the following reasons : (1) two crack fronts are provided to balance the bending forces, thus avoiding rigid body rotation of the specimen; (2) the 1.25 mm grooves on both sides of the specimen

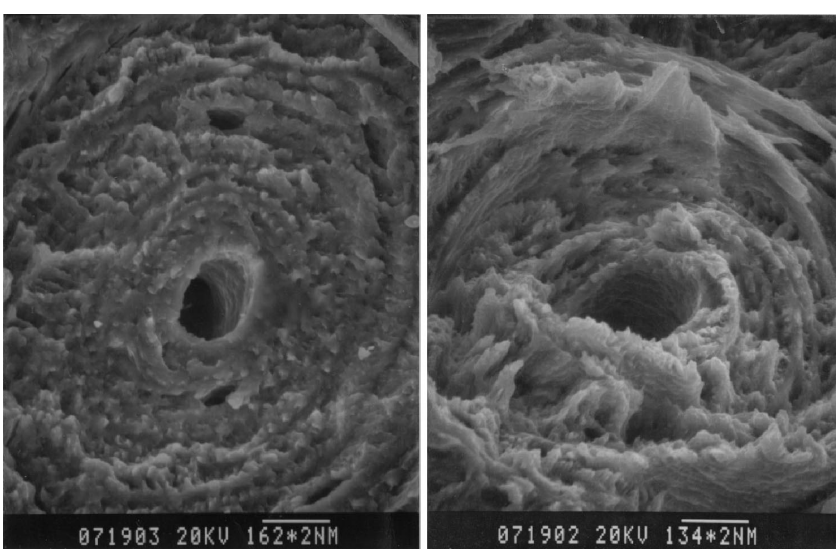

Fig. 4. Fracture surfaces of (a) mode II and (b) mode III specimens (main cracks propagate perpendicular to the longitudinal axis of the mid-diaphysis of the femora).

allow crack propagation before the occurrence of general yield in the cantilever beam arms of the specimen.

The elastic modulus and ultimate strength of cortical bone under shear is much less than that under tension [7]. However, the fracture toughness of material, which reveals the combined effects of strength and ductility, may not be directly proportional to its strength. A material, which is weak in strength, may be tougher in toughness. Our results revealed that the crack initiation fracture toughness of the bone under shear loading was significantly greater than that under tension loading in both longitudinal and transverse fracture. These results are consistent with the results reported by Norman et al. [4], who investigated the resistance of human bone to longitudinal fracture under shear. Furthermore, our study indicated that the fracture toughness of the bone under tear loading was significantly greater than that under tension loading. In summary, both of the fracture toughness of cortical bone under shear and tear are significantly greater than that under tension. Bone exhibit more resistant to crack initiation under shear and tear. The difference between mode I fracture toughness and mode II or mode III fracture toughness of cortical bone is consistent with the theory of fracture behavior of fiber-reinforced composites. In fiber-reinforced composites, the fracture toughness under shear and tear loading are usually expected to be higher than that under tensile loading [18]. In addition, studies have shown that shear toughness is usually greater than tensile toughness for both ductile and brittle composite materials [19]. Bone can be simulated as a composite with oriented arranged osteons as fiber reinforced phase [20] so it behaves in the similar way. The results of this study confirm that the tensile loading condition ahead the tip of microcrack in bone is the most dangerous, which is similar to the fracture behavior of most materials.

The fracture surfaces showed in this investigation are located in the crack growth region for both mode II and mode III tests. In general, a rough and uneven fracture surface indicates more energy consumption during crack propagation than a flat one. This feature was well consistent with the results of the fracture testing. Under shear loading, crack propagated catastrophically as soon as the maximum load was reached in both longitudinal and transverse fracture (Fig. 2). Cracks cut across the osteons and the interstitial system, leaving a flat fracture surface. Whereas under tear loading the bone underwent a considerable process of stead crack propagation before final fracture (Fig. 3). Osteons and lamellae of bone were partially ''pulled-out'' or severely deformed during stable crack propagation. In this case, individual lamellae showed a variety of fracture morphologies. The fracture end of an osteon was irregularly shaped during failure in tear. These results suggest that bone is structurally more similar to a lamellae composites, but with interconnected lamellae [21].

Transverse fracture is one of the most common mode of fracture. In general, cortical bone is stronger in the transverse fracture case [7] because fracture occurs across the predominant osteon direction. Our study revealed that under shear and tear loading bone was tougher in transverse fracture than in longitudinal fracture. In short, bone is not only stronger in the transverse fracture but also tougher in the transverse fracture case. Bone is ''designed'' to resist deformation (higher elastic modulus) and resist crack initiation (higher fracture toughness) in the loading direction parallel to the longitudinal axis of bone. Such data may be relevant in the development of novel analogue composites for bone replacement, for which the achievement of an equal or superior fracture toughness to that of bone is required.

Our study suggests that bone has been ''designed'' to prevent crack initiation in transverse fracture under tension, shear, and tear loading. In addition, bone is weakest under shear, but it is tougher under shear and tear. A further study is being conducted in our laboratory to characterize the effect of bone density and microstructure on its resistance to crack initiation under mixed loading.

5. Conclusions

1. Crack initiation fracture toughness of bone under shear and tear loading is significantly greater than that under tensile loading in both longitudinal and transverse fracture.
2. Crack initiation fracture toughness of bone in transverse fracture is statistically significantly greater than that in longitudinal fracture under tension, shear, and tear. Bone has been ''designed'' to be tougher in the transverse fracture case.

References

[1] T.M. Wright, W.C. Hayes, J. Biomech. 10 (1977) 419.
[2] J.C. Behiri, W. Bonfield, J. Biomech. 15 (1980) 1841.
[3] J.C. Behiri, W. Bonfield, J. Biomech. 17 (1984) 25.
[4] T.L. Norman, S.V. Nivargikar, D.B. Burr, J. Biomech. 29 (1996) 1023.
[5] E.R. Gozna, Biomechanics of Musculoskeletal Injury, Williams and Wilkins, Baltimore, 1982, p. 1.
[6] J.C. Behiri, W. Bonfield, J. Biomech. 22 (1989) 863.
[7] S.C. Cowin, Bone Mechanics, CRC Press, Boca Raton, Florida, 1989, pp. 97–127.
[8] H.A. Richard, Int. J. Fract. 17 (1981) R105.
[9] Z. Feng, J.Y. Rho, I. Ziv, Proceedings of 1995 Bioengineering Conference BED-Vol.29 ASME, Colorado, 1995, pp. 419–420.
[10] A.M. Kumar, J.P. Hirth, R. Hoagland, X. Feng, J. Test. Eval. 22 (1994) 327–334.
[11] Z. Feng, A. Salzman, Proceedings of 19th Annual Meeting of American Society of Biomechanics, Stanford University, California, 1995, pp. 139–140.
[12] T.L. Norman, D. Vashishth, D.B. Burr, J. Biomech. 25 (1992) 1489–1492.

[13] N. Iosipescu, J. Mater. 2 (1967) 537–566.
[14] D.L. Jones, D.B. Chisholm, Eng. Fract. Mech. 7 (1975) 261–270.
[15] M. Manoharan, J.P. Hirth, A.R. Rosenfield, J. Test. Eval. 18 (1990) 106–114.
[16] M.L. Shaw, J. Compos. Technol. Res. 15 (1993) 193–201.
[17] W. Bonfield, J. Biomech. 20 (1987) 1071–1081.
[18] J.M. Mahishi, Eng. Fract. Mech. 25 (1986) 197–228.
[19] N. Sela, O. Ishai, Composites 20 (1989) 423–435.
[20] S.C. Cowin, in: G.J. Dvorak (Ed.), Mechanics of Composite Materials AMD-Vol. 58 ASME, New York, 1983, p. 1.
[21] G. Corondan, W.L. Haworth, J. Biomech. 19 (1986) 207–218.